https://doi.org/10.33472/AFJBS.6.6.2024.7422-7441

African Journal of Biological Sciences

Journal homepage: http://www.afjbs.com

Research Paper Open Access

Advanced Hydrogel Formulations and Evaluation for Improved Carboplatin Delivery in Cancer Treatment

Swasti Arora[1], Arijit Mallick[2], Prasanthi Pakalapati[3*], Sutar Vijay Gautam[4], Aboli M.Nirwane[5], Mr.Kunal[6], Phanse Milind Dilip[7], Sujit Vitthal Abhang[8]

[1]Faculty of Pharmacy, Swami Vivekanand Subharti University, Meerut, Pin -250005.
[2]Department of Pharmaceutics, Seacom Skills University Kendradangal, Bolpur, District, Birbhum, West Bengal, India, PIN: 731236.
[3]Department of Pharmaceutics, Aditya College of Pharmacy, Surampalem, Kakinada, India
[4,5]Department of Pharmaceutics, SSJP'S R P College of Pharmacy Dr. Vedprakash Patil Educational Campus Gadpati, Alani, Dharashiv, 413501.
[6]R.P. Educational Trust Group of Institutions (Bastara), Karnal Haryana Pin code – 132114.
[7,8]Department of Pharmaceutics, Arvind Gavli College of Pharmacy Jaitapur,Satara. Pin-415004.

Corresponding Author
Prasanthi Pakalapati*
Department of Pharmaceutics, Aditya College of Pharmacy, Surampalem, Kakinada, India

Article Info

Volume 6, Issue 6, July 2024

Received: 31 May 2024

Accepted: 28 June 2024

Published: 22 July 2024

doi: 10.33472/AFJBS.6.6.2024.7422-7441

ABSTRACT:

The aim of this study was to create chemically cross-linked chondroitin sulfate-co-poly (methacrylic acid) hydrogels (CSH hydrogels) designed for pH-responsive delivery of Carboplatin (CARBP) to the colon. These hydrogels were synthesized using free radical polymerization, where chondroitin sulfate (CS) was cross-linked with methacrylic acid (MAA) in an aqueous solution. Ammonium peroxodisulfate (APS) served as the initiator, and N, N-methylene bisacrylamide (MBA) acted as the cross-linker. The hydrogels were then loaded with CARBP. To characterize the polymeric system, techniques such as FTIR, TGA, DSC, and XRD were employed. Scanning electron microscopy (SEM) was used to examine the surface morphology of the hydrogels. The pH-sensitive properties of the hydrogels were assessed through swelling dynamics and equilibrium swelling ratio at different pH levels. These assessments confirmed the formation of a new polymeric network. Formulations with higher CS content exhibited maximum swelling at pH 7.4. Additionally, high Carboplatin loading and increased drug release were observed at pH 7.4. The study concludes that a stable polymeric network of chondroitin sulfate and methacrylic acid has been successfully created, offering potential as a delivery system for targeting Carboplatin to the colon in colorectal cancer treatment.

Keywords: Carboplatin**,** Chondroitin sulfate, Methacrylic acid, Anticancer, Hydrogels.

1. INTRODUCTION

Hydrogels are three-dimensional, hydrophilic polymer networks capable of holding a significant amount of water while maintaining their structure due to physical or chemical cross-linking of individual polymer chains. These materials have garnered significant interest in biomedical fields, particularly in drug delivery, due to their unique properties such as high-water content, biocompatibility, and tunable mechanical strength. The use of hydrogels in drug delivery systems offers numerous advantages that address several challenges associated with conventional drug delivery methods (Mostakhdemin et al., 2021, Morris et al., 2021, Mondelo-García et al., 2021). One of the primary advantages of hydrogels in drug delivery is their ability to provide controlled and sustained release of therapeutic agents. Hydrogels can be engineered to release drugs at a specific rate over a prolonged period, thereby maintaining the drug concentration within the therapeutic window for extended durations. This controlled release mechanism is particularly beneficial for treating chronic conditions that require long-term medication administration, reducing the frequency of drug administration and improving patient compliance. Another significant advantage of hydrogels is their biocompatibility and biodegradability. Hydrogels are often composed of natural polymers such as alginate, chitosan, and gelatin, or synthetic polymers like polyethylene glycol (PEG) and polyvinyl alcohol (PVA).

These materials are generally non-toxic and can be designed to degrade into biocompatible by-products that are easily eliminated from the body. This property minimizes the risk of adverse reactions and complications associated with the drug delivery system, ensuring patient safety (Momin and Afreen, 2021, Mokhtari et al., 2021, Mo et al., 2021b, Mo et al., 2021a).

Hydrogels also possess the ability to respond to environmental stimuli, which can be exploited for targeted drug delivery. These "smart" hydrogels can undergo changes in their physical or chemical properties in response to variations in pH, temperature, ionic strength, or the presence of specific enzymes. For instance, a hydrogel designed to respond to the acidic environment of a tumor site can release its drug payload specifically at the site of the tumor, minimizing systemic side effects and enhancing the therapeutic efficacy of the drug. The high water content of hydrogels contributes to their excellent biocompatibility and ability to mimic natural tissues, making them ideal for a variety of biomedical applications. In drug delivery, the hydrated network of hydrogels can protect sensitive drugs, such as proteins and nucleic acids, from degradation before they reach their target site. This protective mechanism is particularly important for delivering biologics that are prone to denaturation or enzymatic degradation. Additionally, hydrogels can be fabricated in various forms, including nanoparticles, microspheres, films, and injectable gels, offering versatility in their application. Injectable hydrogels, for example, can be administered via minimally invasive procedures and conform to the shape of the target tissue, providing localized and sustained drug release. This adaptability allows for the development of personalized medicine approaches, where the drug delivery system can be tailored to meet the specific needs of individual patients (Misra and Acharya, 2021, Miljković et al., 2021, Liu et al., 2021, Lin et al., 2021b, Lin et al., 2021a).

Furthermore, the porous structure of hydrogels enables high drug loading capacity and the potential for co-delivery of multiple therapeutic agents. This feature is particularly advantageous for combination therapies, where multiple drugs are required to work synergistically to achieve the desired therapeutic outcome. The hydrogel matrix can be engineered to release different drugs at different rates, optimizing the therapeutic regimen and improving treatment efficacy. In summary, hydrogels offer a versatile and effective platform for drug delivery, with numerous advantages including controlled and sustained release, biocompatibility, responsiveness to environmental stimuli, protection of sensitive drugs, and the ability to be fabricated in various forms. These properties make hydrogels a promising tool in the development of advanced drug delivery systems, addressing many limitations of conventional drug delivery methods and enhancing the overall therapeutic outcomes for patients. The continued research and development of hydrogel-based drug delivery systems hold great potential for improving the treatment of a wide range of diseases and medical conditions (Misra and Acharya, 2021, Miljković et al., 2021, Liu et al., 2021, Lin et al., 2021b, Lin et al., 2021a).

Carboplatin is a platinum-based chemotherapeutic agent widely used in the treatment of various cancers, including ovarian, lung, and testicular cancers. Despite its efficacy, the clinical application of carboplatin is often associated with significant side effects and limitations, such as nephrotoxicity, myelosuppression, and poor targeting efficiency. Developing hydrogels as a delivery system for carboplatin offers a promising approach to overcome these challenges and enhance the therapeutic potential of the drug. The rationale for creating hydrogels for carboplatin delivery is grounded in several key advantages offered by this technology. One of the primary reasons for using hydrogels in carboplatin delivery is their ability to provide controlled and sustained release of the drug. Hydrogels can be engineered to release carboplatin at a predetermined rate over an extended period, ensuring a consistent therapeutic concentration of the drug in the target tissue (Lima and Passos, 2021, Lima et al., 2021, Li et al., 2021a). This controlled release mechanism minimizes the frequency of administration, potentially reducing the side effects associated with peak plasma concentrations and improving patient compliance.

Sustained release also helps maintain the drug's efficacy over longer durations, enhancing its therapeutic impact. Hydrogels can be designed to target specific tissues or tumors, thereby increasing the local concentration of carboplatin at the site of action while minimizing its systemic distribution. This targeted delivery reduces the exposure of healthy tissues to the toxic effects of carboplatin, significantly decreasing the incidence of adverse side effects such as nephrotoxicity and myelosuppression. The incorporation of targeting ligands or responsive elements into the hydrogel matrix can further refine this targeting capability, allowing for precise delivery to the tumor microenvironment.

Hydrogels are often composed of biocompatible and biodegradable materials, such as natural polymers (e.g., alginate, chitosan) or synthetic polymers (e.g., polyethylene glycol, polyvinyl alcohol). These materials are generally non-toxic and can degrade into harmless by-products that are easily eliminated from the body. This biocompatibility ensures that the hydrogel delivery system does not elicit significant immune responses or toxicity, making it safe for clinical use (Lima and Passos, 2021, Lima et al., 2021, Li et al., 2021a). The hydrogel matrix can protect carboplatin from premature degradation and inactivation before it reaches the target site. This protection is particularly important for maintaining the stability and potency of carboplatin in the biological environment. Encapsulating carboplatin within a hydrogel can shield it from enzymatic activity and other destabilizing factors, ensuring that a higher fraction of the administered dose reaches the tumor intact. Hydrogels can be fabricated in various forms, including injectable gels, films, and nanoparticles, providing versatility in their application. Injectable hydrogels, for example, can be administered minimally invasively and can conform to the shape of the tumor or tissue defect, providing localized and sustained drug release. This adaptability allows for personalized treatment regimens tailored to the specific needs of individual patients (Kim et al., 2021, Khosravimelal et al., 2021, Khiabani et al., 2021, Khayambashi et al., 2021).

The porous structure of hydrogels allows for high drug loading capacity and the co-delivery of multiple therapeutic agents. This feature is particularly advantageous for combination therapies, where carboplatin can be delivered alongside other chemotherapeutic agents or adjunctive therapies to enhance treatment efficacy. The hydrogel matrix can be engineered to release different drugs at different rates, optimizing the therapeutic regimen. The development of hydrogels for carboplatin delivery offers a strategic approach to enhance the therapeutic efficacy and safety of this chemotherapeutic agent. By leveraging the controlled release, targeting capabilities, biocompatibility, and versatility of hydrogels, it is possible to address the limitations of conventional carboplatin therapy (Kim et al., 2021, Khosravimelal et al., 2021, Khiabani et al., 2021, Khayambashi et al., 2021). This innovative drug delivery system holds promise for improving cancer treatment outcomes and patient quality of life, making it a compelling area for further research and development. Therefore, this present study aimed to design and evaluate the Chondroitin Sulfate-Co-Poly-(Methacrylic Acid) hydrogels for anticancer Carboplatin drug delivery.

2. MATERIAL AND METHODS

Chemicals

Carboplatin (CARBP) was obtained as gift sample from Kaprishi Pharma, Baddi, India. Chondroitin sulfate (CS), methacrylic acid (MAA), N, N-methylene bisacrylamide (MBA), and ammonium peroxodisulfate (APS) were procured from Sigma Aldrich, Mumbai, India. Fresh deionized distilled water was prepared in our laboratory.

Synthesis of Chondroitin Sulfate-co-poly (Methacrylic acid) Hydrogels

The free radical polymerization method was employed to develop various formulations, as detailed in Table 1. A measured amount of chondroitin sulfate (CS) was dissolved in water with

continuous stirring on a magnetic stirrer, maintaining the reaction mixture at 55°C until a transparent solution was achieved. The reaction mixture was purged with nitrogen for 25 minutes to remove dissolved oxygen. Subsequently, a weighed amount of ammonium peroxodisulfate (APS) was added to the clear polymer (CS) solution. Methacrylic acid (MAA) was then added dropwise to the chondroitin sulfate solution at 55°C. The required amount of cross-linker (N, N-methylene bisacrylamide, MBA) was weighed and added to the reaction mixture. The resulting transparent solution was carefully transferred into glass test tubes and incubated in a water bath at 60°C for 1.5 hours, 65°C for 3.5 hours, and 70°C for 10 hours. After 10 hours, the test tubes were cooled to room temperature, and the cylindrical hydrogels were cut into small discs (7.5 mm in length). The unreacted components were removed from the discs by washing them with a 80:20 ethanol-water mixture. Initially, the discs were air-dried in a laminar flow hood for 24 hours, followed by drying in a vacuum oven at 42°C for 4 days {Wang, 2003 #24990}.

Table 1. Formulation composition table

Sr. No.	Formulations	CS (g/100g)	MAA (g/100g)	APS (g/100g)	MBA (g/100g)
1	CSH-1	0.8	24	0.24	0.2
2	CSH-2	1.6	24	0.24	0.2
3	CSH-3	2.4	24	0.24	0.2
4	CSH-4	0.8	16	0.24	0.2
5	CSH-5	0.8	24	0.24	0.2
6	CSH-6	0.8	32	0.24	0.2
7	CSH-7	0.8	24	0.24	0.2
8	CSH-8	0.8	24	0.24	0.4
9	CSH-9	0.8	24	0.24	0.6

Characterization of Formulations

FTIR Study

FTIR spectra were recorded for pure chondroitin sulfate, methacrylic acid, Carboplatin, methylene bisacrylamide, and both drug-loaded and unloaded hydrogel discs. The hydrogel samples were thoroughly crushed using a pestle and mortar and analysed by attenuated total reflectance ATR-FTIR (Bruker, Germany) in the range of 4000–600 cm^{-1}.

Thermogravimetric analysis (TGA) and Differential Scanning Calorimetry (DSC) study

Thermal analysis (TA) was performed using thermogravimetric analysis (TGA) with TA Instruments and differential scanning calorimetry (DSC) with TA Instruments (Q6K series). The hydrogel samples were crushed and sieved through a 40-mesh to obtain the required particle size. For TGA, samples weighing between 1-6 mg were placed in an open platinum pan (100 - 200 µl) attached to a microbalance. The samples of chondroitin sulfate (CS), methacrylic acid (MAA), and formulations were heated from 25°C to 500°C under dry nitrogen. For DSC, samples of CS and formulations weighing between 0.4-4 mg were accurately weighed into aluminum pans and analyzed under nitrogen gas, heating from 25°C to 500°C at a rate of 25°C/min {Wang, 2003 #24990}.

The powder X-ray diffraction (PXRD)

The powder X-ray diffraction (PXRD) pattern was measured using a Bruker powder diffractometer instrument (Bruker, Germany) at room temperature. Crushed samples were placed on a plastic sample holder, and the surface was levelled with a glass slide. The samples were analyzed over a range of 6-60° 2θ at a rate of 1° 2θ/min, utilizing a copper Kα radiation source with a wavelength of 1.631 Å and 1.1 mm slits {Wang, 2003 #24990}.

Morphology and Characterization of Hydrogel Formulations

Surface Morphology

The surface morphology of the hydrogel formulations was examined using scanning electron microscopy (SEM) with a Quanta SEM (Cambridge, UK). Fully dried hydrogel discs were cut to optimal sizes and fixed onto a double-adhesive tape attached to an aluminum stub. These stubs were then coated with a thin layer of gold (~300 Å) under an argon atmosphere using a gold sputter module in a high-vacuum evaporator. The coated samples were randomly scanned, and photomicrographs were taken to reveal the surface morphology {Wang, 2003 #24990}(Aminabhavi et al., 2014, Alvarez-Lorenzo and Concheiro, 2014, Alvarado-Velez et al., 2014).

Determination of Gel%, Yield%, and Gel Time

Gel%, yield%, and gel time were calculated to estimate the amount of reactants polymerized during the preparation of the formulations. Dried hydrogels (initial weight m_i) were immersed in water for 7 days with occasional shaking to separate the water-soluble parts from the formulations. The water-insoluble parts were then dried in a vacuum oven to a constant weight (m_d) (Ahmed, 2015, Calixto et al., 2014). Gel% and yield% were calculated using the following formulas:

$$Gel\% = \frac{m_d}{m_i} \times 100$$

$$Yield\% = \frac{m_d}{m_c} \times 100$$

where m_c is the total weight of the prepared hydrogels.

Swelling Behaviour of Hydrogels

Swelling studies were conducted to analyze the pH sensitivity of the hydrogels. Dried hydrogel discs were weighed and immersed in 0.1 M HCl (pH 1.2) and phosphate buffer solutions (pH 7.4) at 37°C. At specific time intervals, the samples were removed, and excess water was blotted off with filter paper before weighing. The degree of swelling (Q_t) at time t t was calculated using the following formula (Männel et al., 2021, Li et al., 2021b, Kim and Woo, 2021, Khalesi et al., 2021, Keskin et al., 2021, Nonoyama and Gong, 2015, Calixto et al., 2014, Cai et al., 2014):

$$Q_{t=}\frac{m_{t-m_o}}{m_o}$$

Where 'mo' is initial weight of dried disc, namely weight at t = 0, and 'mt' is weight after time 't' and 'Qt' is weight of water intake at a time 't'. Equilibrium swelling 'Q∞'is calculated by following formula (Samanta and Ray, 2014).

$$Q_{\infty=}\frac{m_{t-m_o}}{m_o}$$

Drug Entrapment

Carboplatin (CARBP) was loaded into the prepared hydrogels using the diffusion and absorption method. Dried CS-co-poly (MAA) hydrogel discs (8 mm) were immersed in 100 ml of 1.0% CARBP solution in phosphate buffer (pH 7.4) for 48 hours at room temperature. The higher pH solvent, where the drug had maximum solubility and higher swelling, was chosen. After 48 hours, the discs were washed with distilled water, briefly dried at room temperature, and then placed in an oven at 40°C. The CARBP loading in the hydrogel discs was measured by extracting a weighed amount of the polymer using the same solvent for drug loading. This extraction process was repeated with 25 ml of fresh buffer solution until no drug was detected in the buffer solution. A calibration curve of CARBP dilutions in the buffer was plotted to analyse the drug content via UV-Vis spectrophotometry (UV-1601 Shimadzu),

performed at a UV wavelength (λ max) of 205 nm (Sghier et al., 2024, Sarkar et al., 2024, Saberian and Abak, 2024).

Drug Release Study

Drug release was evaluated at low and high pH values to check pH-dependent delivery of CARBP from CS-co-poly(MAA) hydrogel system. Drug loaded hydrogel discs were assessed for CARBP release in 900 ml solutions of pH 1.2 and 7.4 by USP dissolution apparatus-II at temperature 37 ± 0.5°C. These samples were evaluated at wavelength (λmax) 205 nm using UV-Vis spectrophotometer (UV-1601Shimadzu) (Sghier et al., 2024, Sarkar et al., 2024, Saberian and Abak, 2024).

Release Kinetic Study of Carboplatin

The mechanism of Carboplatin release from the hydrogel was studied using kinetic models applied to dissolution data, determining the best fit model to describe the drug release mechanism. Four kinetic models were utilized to observe the release pattern of the drug as a function of time and the pH of the dissolution media. The zero-order release model indicates that the drug release is independent of its concentration in the hydrogel disc. The first-order release model suggests that drug release from the hydrogel network system depends on the amount of drug in the dosage form. Higuchi's model, based on Fick's law, describes the drug release process, while the Korsmeyer-Peppas model provides insight into the relationship between the structural and polymeric network characteristics of the hydrogels. According to the Korsmeyer-Peppas model, the release exponent (n) helps classify the release mechanism: Fickian diffusion when $n \leq 0.45$, non-Fickian transport for $0.45 < n < 0.89$, and case-II relaxation or super case-II transport when $n > 0.89$ (Männel et al., 2021, Li et al., 2021b, Kim and Woo, 2021, Khalesi et al., 2021, Keskin et al., 2021, Nonoyama and Gong, 2015, Calixto et al., 2014, Cai et al., 2014).

Statistical analysis

GraphPad Prism was utilised for the analysis, ANOVA followed by Dunnett's test was performed to compare multiple experimental groups against a control group. Data were presented as mean ± standard deviation (SD), with a significance level set at $p < 0.05$. GraphPad Prism's robust analytical and graphical tools make it a preferred choice for comprehensive statistical evaluations in research.

3. RESULTS AND DISCUSSION

Physical Appearance of Hydrogels

Polymerization of CS with MAA after the crosslinking, stable polymeric hydrogel system were formulated. Hydrogel discs with higher MAA concentration showed glass like transparent appearance with yellow color after drying in oven while hydrogel discs with low MAA contents revealed yellowish white characteristics. A tremendous mechanical strength was found in hydrogel discs that retained the shape even after swelling. Hydrogels discs with high MAA ratio revealed higher mechanical strength than hydrogels discs with higher polymer (CS) contents. Physical appearance of prepared hydrogels have been shown in Figure 1.

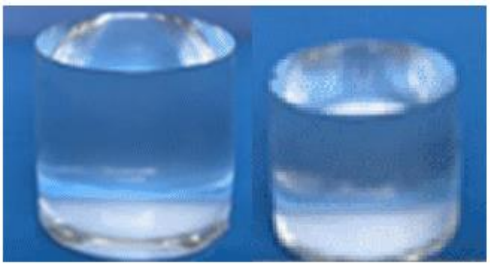

Figure 1. The hydrogel formulation

FTIR Analysis

FTIR spectra for chondroitin sulfate (CS), methacrylic acid (MAA), N-N, methylene bisacrylamide (MBA), Carboplatin (CARBP), and both unloaded and drug-loaded CSH hydrogels were analyzed within the range of 4000 cm^{-1} to 600 cm^{-1}. The pure CS spectrum exhibited -OH and N-H stretching at 3351 cm^{-1}, amide bands at 1611 cm^{-1}, and carboxyl group vibrations at 1419 cm^{-1} and 1381 cm^{-1}. It also showed S=O stretching at 1244 cm^{-1} and C-O stretching at 1030 cm^{-1}. The MAA spectrum indicated methyl C-H stretching at 2932 cm^{-1}, carboxylic acid groups between 1729–1750 cm^{-1}, and C=C stretching at 1641 cm^{-1}. MBA displayed N-H stretching at 3322 cm^{-1}, with N-H and C=O stretching frequencies between 1561–1723 cm^{-1}. CARBP exhibited N-H bending at 878 cm^{-1}, C=O stretching at 1675 cm^{-1} and 1733 cm^{-1}, and N-H stretching at 3072 cm^{-1}. The FTIR spectra of the cross-linked CSH hydrogels showed characteristic peaks indicating the formation of new cross-linked groups and a grafted copolymer network. Broad peaks between 3450 cm^{-1} to 3050 cm^{-1} indicated O-H and N-H stretching, while peaks at 1699 cm^{-1} and 1465 cm^{-1} indicated carboxylic acid and COO symmetry stretching, respectively. The S=O stretching at 1262 cm^{-1} confirmed the formation of the CS-co-poly(MAA) hydrogels. The presence of CARBP in loaded hydrogels was confirmed by major peaks at 1733 cm^{-1}, 1721 cm^{-1}, and 2935 cm^{-1}, with minor shifts indicating the entrapment of CARBP in the polymeric network. These results are consistent with previous studies of chondroitin sulfate-based formulations and confirm the successful fabrication of the hydrogels.

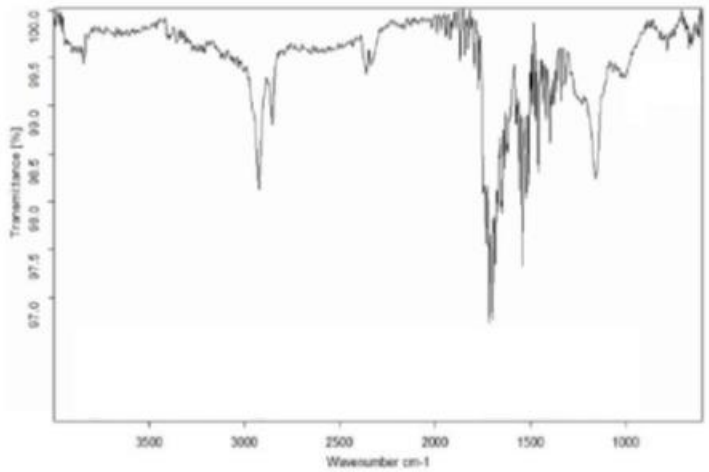

Figure 2. FTIR Spectra of drug loaded chondroitin sulfate-co-poly(methacrylic acid) hydrogel (CSH)

Differential scanning calorimetry (DSC) and thermogravimetric analysis (TGA)

Differential scanning calorimetry (DSC) and thermogravimetric analysis (TGA) were conducted to evaluate the thermal stability of the chondroitin sulfate-co-poly(methacrylic acid) (CSH) hydrogel. The DSC curves for pure chondroitin sulfate (CS) showed endothermic peaks between 35 and 125°C due to the loss of volatile components and chain relaxation, with a strong exothermic peak at 247°C indicating polysaccharide degradation. The CSH hydrogel displayed endothermic peaks from 35 to 135°C, indicating moisture loss and polymer chain breakage, and broader endothermic peaks from 185 to 285°C due to the degradation of carboxylate and sulfate groups. An exothermic peak between 285 and 395°C suggested the glass transition temperature (Tg), and another endothermic peak from 395 to 500°C indicated complete decomposition of the hydrogel, showing greater stability than the individual polymer components. TGA of pure CS showed a five-stage weight loss: 25% at 47-97°C, 15% at 110-210°C, 7% at 215°C, 25% at 215-260°C, and 7% at 265-355°C, attributed to the degradation

of carboxylate and sulfonate groups. The CSH hydrogel exhibited delayed weight loss in three stages: 15% at 125-190°C due to water and methacrylic acid loss, 65% at 195-415°C, and 35% at 425-575°C, indicating higher thermal stability. Compared to pure CS, the CSH hydrogel showed enhanced thermal stability due to cross-linking, with degradation occurring at higher temperatures. This increased thermal stability suggests that the cross-linking between CS and MAA significantly improves the thermal properties of the hydrogel.

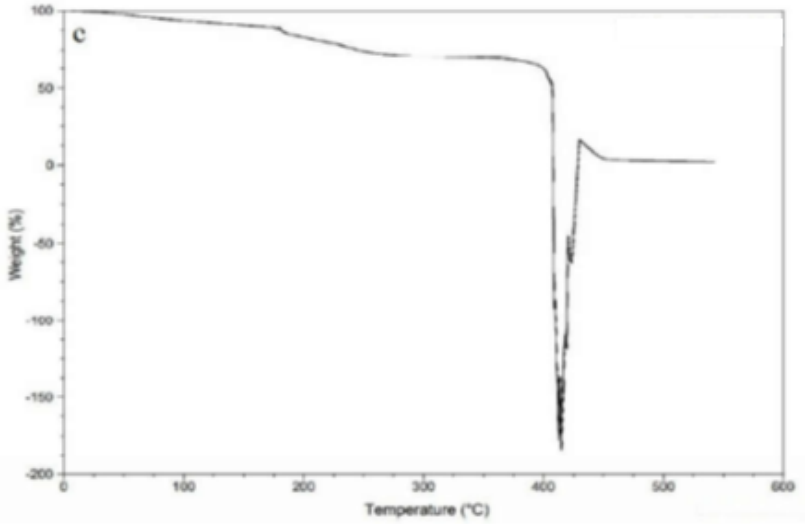

Figure 3. TGA of chondroitin sulfate-co-poly(methacrylic acid) (CSH)

Scanning Electron Microscopy (SEM)

Samples of cross-linked polymer network were analyzed by scanning electron microscopy (SEM) in order to evaluate the modification of surface morphology and superficial profiles. Figures 4 were obtained for intact morphological studies of hydrogels at different magnifications (×500 &×1000) attributing to wavy, shiny and solid outer surface with porosity on it. Results showing the existence of weak attraction forces between polymer and monomer which revealed less dense structure across the entire investigated sample and confirmed good compatibility among reactants (CS & MAA).

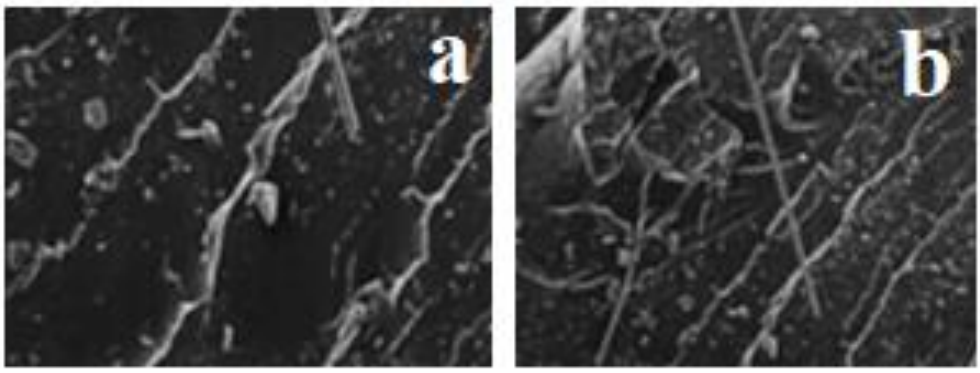

Figure 4. Scanning electron microscopy (SEM) of cross-linked polymer network (CSH) at different magnifications.

The Powder X-Ray Diffractometry (PXRD)

PXRD patterns of pure chondroitin sulfate (CS) and CSH hydrogels were recorded and presented in Figures 5. The PXRD pattern of pure CS showed no diffraction peaks, confirming its amorphous nature. In contrast, the CSH hydrogel displayed distinct diffraction peaks at 2θ

angles of 12.2°, 17.1°, 17.4°, and 18.6°, indicating the crystallinity of the newly formed polymeric hydrogel composite. Additionally, sharp peaks at 2θ angles of 23.2°, 25.7°, and 45.2° further confirmed the crystalline characteristics of the developed formulation. The presence of both amorphous and crystalline features in the CSH hydrogel, with peaks in the 2θ range of 34.7°-38.45° and 38.2°-43.9°, demonstrated the successful polymerization of CS and methacrylic acid (MAA), resulting in a hydrogel with enhanced crystallinity.

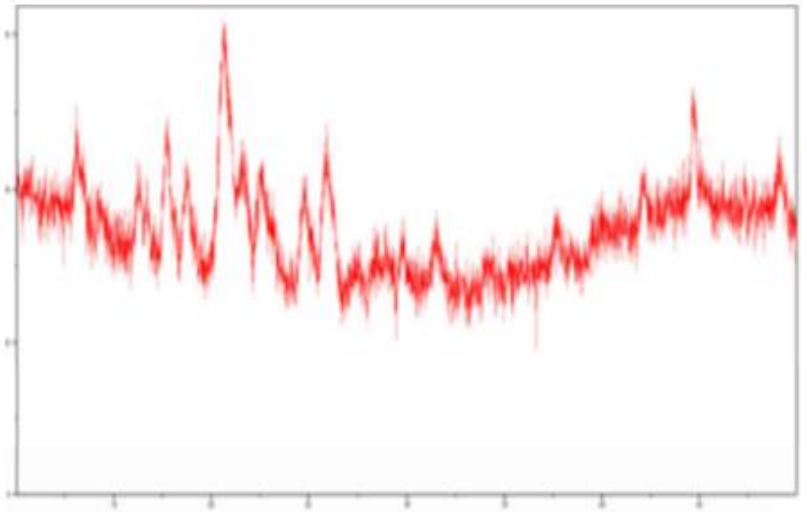

Figure 5. PXRD of chondroitin sulfate (CS) and prepared hydrogel (CSH)

Effect of reaction contents on gel %, yield % and gel time of developed hydrogel

The effect of polymer, monomer and cross-linker contents on gel content (%), yield (%) and gel time of CSH hydrogels is showed in Figures 6. For understanding the effect of one variable, other variables were kept constant. An increase in gel%, yield% and gel time was observed with an increased concentration of chondroitin sulfate (CS) wt% in the formulation. In a series of polymeric hydrogels (CSH-1 to CSH-3), gel %increased as CS content was increased because it becomes difficult for less amount of N,N-methylene bisacrylamide (MBA) to crosslink polymeric chain with monomer (MAA). In the same manner, yield% was also increased with increase in amount of CS in the developed polymeric system which shows effect of CS concentration on crosslinking density as shown in Figure 6. Similarly, with increasing monomer content in formulations (CSH-4 to CSH-6), increased yield% and gel% were observed but gel time was decreased as shown in figure 6. An increase in gel% and yield % may be attributed to the presence of large number of active primary radicals at higher monomer content while gel time was decreased due to an increased reaction rate and early entanglement of monomer and polymer chains.

On the contrary, concentration of cross-linker was increased in formulations (CSH-7 to CSH-9) and it was observed that with increase in cross-linker concentration, gel time was decreased while yield% and gel% were increased. With increase in crosslinker, gel time decreased due to formation of polymeric network occurred at a much faster rate in the presence of increased quantity of MBA. Similarly, yield% and gel% were increased due to increase in rate of polymeric reaction in the presence of increased amount of reactant (cross-linker). Samanta and Ray observed effects of reactant contents on gel%, yield% and gel time by different monomer and polymer. They depicted higher gel% and yield% with higher concentrations of polymers and monomers as our findings.

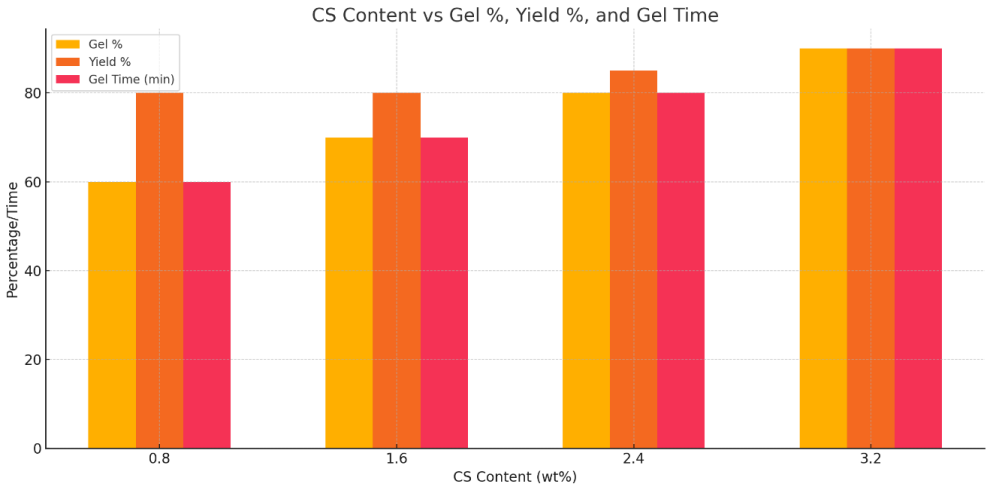

Figure 6. Effect of Chondroitin sulfate (CS) concentration on gel%, yield% and gel time

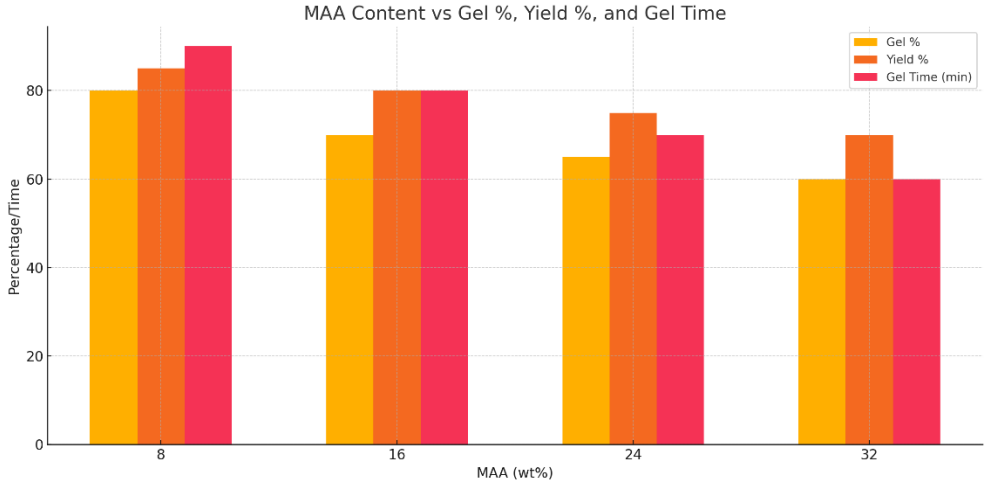

Figure 7. Effect of methacrylic acid (MAA) concentration on gel%, yield% and gel time

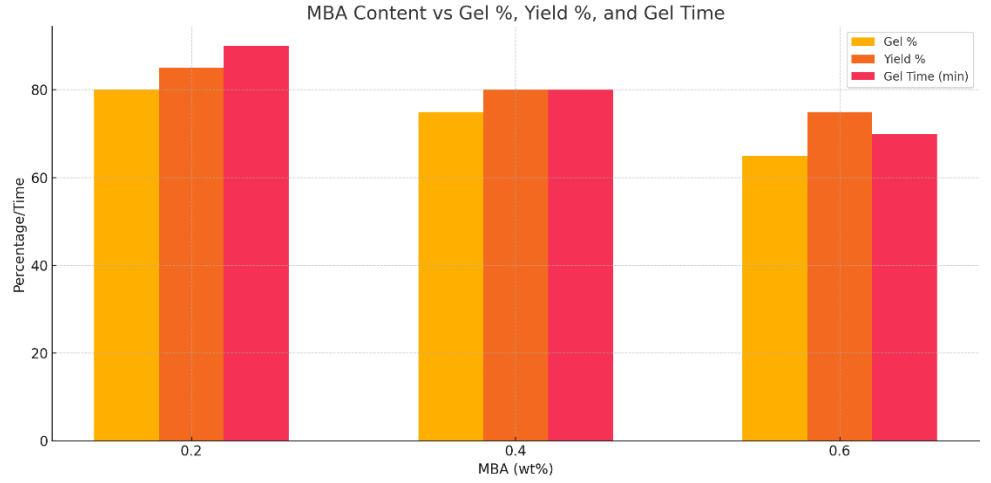

Figure 8. Effect of methylene bisacrylamide (MBA) concentration on gel%, yield% and gel time

Effect of Polymer, Monomer, and Cross-Linker on Swelling

Prepared hydrogels exhibited pH-sensitive swelling behavior at different pH levels (1.2 and 7.4). Three sets of formulations were created to assess the effects of varying concentrations of

polymer (CS), monomer (MAA), and cross-linker (MBA) on the dynamic swelling (Qt) and equilibrium swelling (Q∞) of the hydrogels. The formulations CSH-1 to CSH-3 increased the polymer (CS) concentration, CSH-4 to CSH-6 increased the monomer (MAA) concentration, and CSH-7 to CSH-9 increased the cross-linker (MBA) concentration.

In formulations CSH-1 to CSH-3, the swelling behavior increased with higher CS content due to the ionization of functional groups like hydroxyl (-OH), sulfonic (-SO3-), and carboxylic (-COOH) groups at high pH, leading to electrostatic repulsion and enhanced swelling. Conversely, formulations CSH-4 to CSH-6, with higher MAA concentrations, formed more compact and dense networks with reduced porosity and hydration, resulting in decreased swelling. This reduction in swelling is attributed to higher cross-linking between monomers and polymers, which restricts the swelling capacity.

In formulations CSH-7 to CSH-9, increased MBA concentration led to less dynamic swelling due to the increased cross-linked density, which restricts the segmental mobility of the polymeric chains. Various studies have shown that higher MBA concentrations result in reduced swelling due to the enhanced cross-linking density, which aligns with the observed decrease in swelling behaviour in these hydrogels.

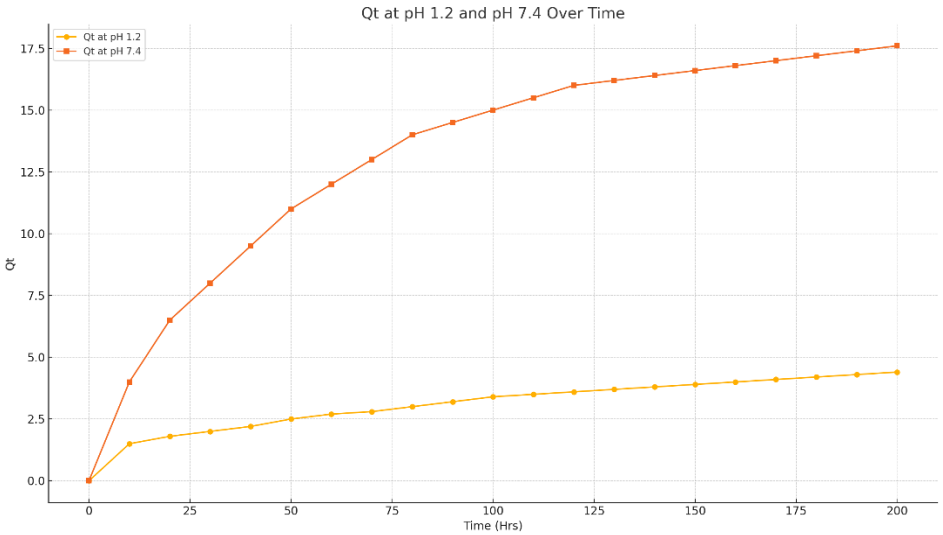

Figure 9. Effect of different pH mediums on dynamic swelling

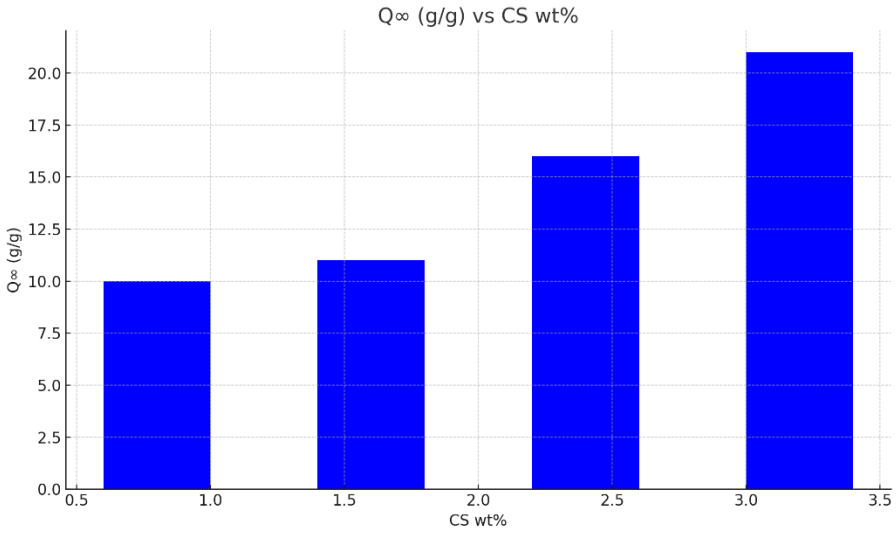

Figure 10. Effect of CS contents (wt%) on dynamic swelling

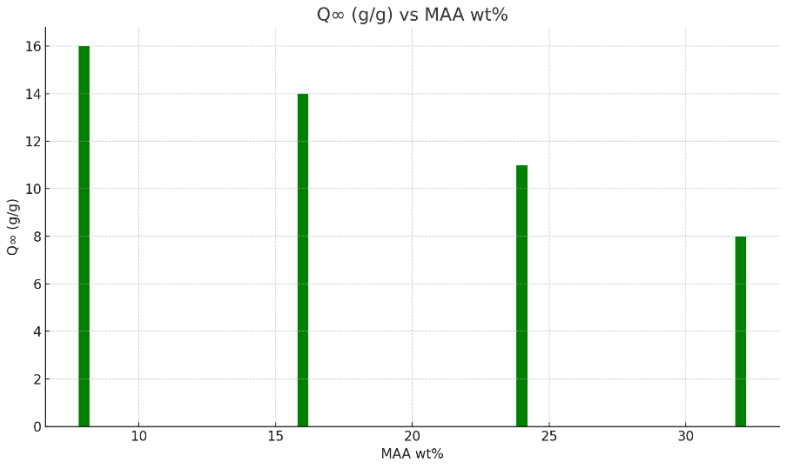

Figure 11. Effect of MAA contents (wt%) on dynamic swelling

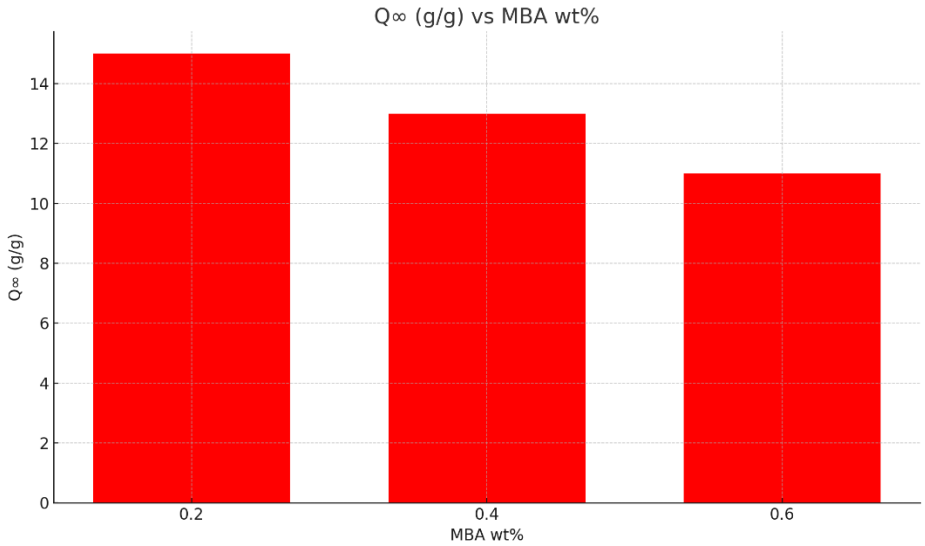

Figure 12. Effect of MBA contents (wt%) on dynamic swelling

Drug Entrapment

The drug entrapment efficiency of CSH hydrogels was successfully demonstrated, as shown in Figures 13. The entrapment is closely related to the water uptake capacity of the polymeric network. Drug loading is influenced by the pH of the medium, with higher entrapment observed at pH 7.4 due to the ionization of carboxylic, hydroxyl, and sulfonate groups in the CSH chains. At higher pH levels, increased deprotonation of hydroxyl and carboxyl groups leads to greater electrostatic repulsion among negatively charged groups, resulting in higher water absorbency. Consequently, increased water uptake in the hydrogels enhances drug entrapment within the polymeric network. In the study, increasing the concentration of polymers resulted in higher swelling and drug entrapment, as shown in Figure 3.9 (a). However, increasing the ratios of monomer and cross-linker led to reduced water uptake and drug entrapment, as depicted in Figures 3.9 (b-c). Similar findings were reported by Oprea and colleagues, who prepared chondroitin sulfate and cellulose-based hydrogels, demonstrating that theophylline entrapment and release from the polymeric network were comparable to the entrapment and release of Carboplatin (CARBP) from CSH hydrogels due to higher water absorbency (Oprea et al., 2012).

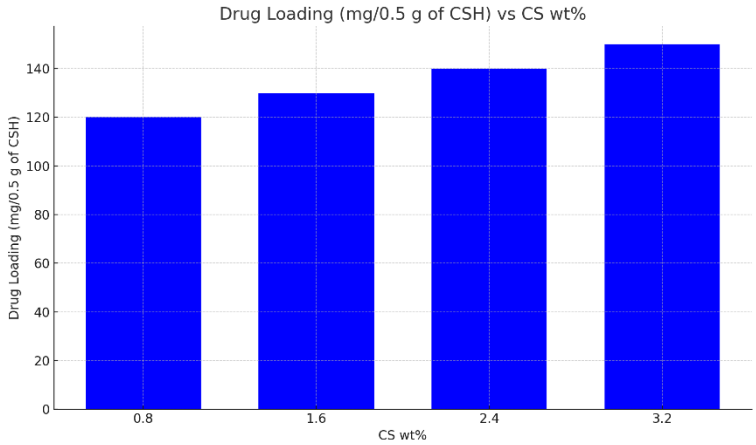

Figure 13. Effect of chondroitin sulfate (CS) on drug loading

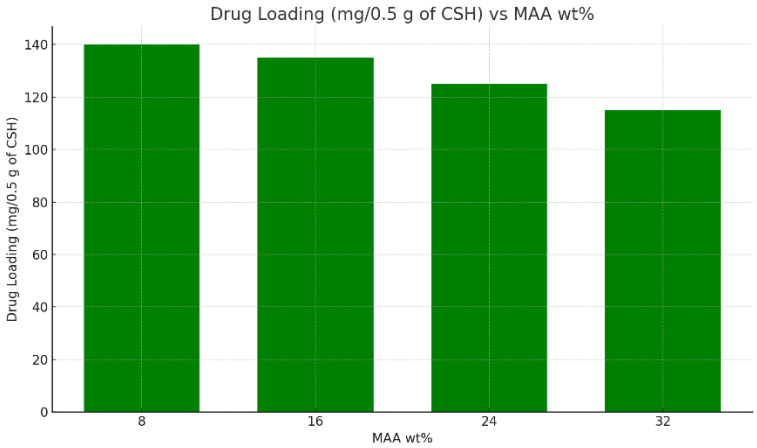

Figure 14. Effect of methacrylic acid (MAA) on drug loading

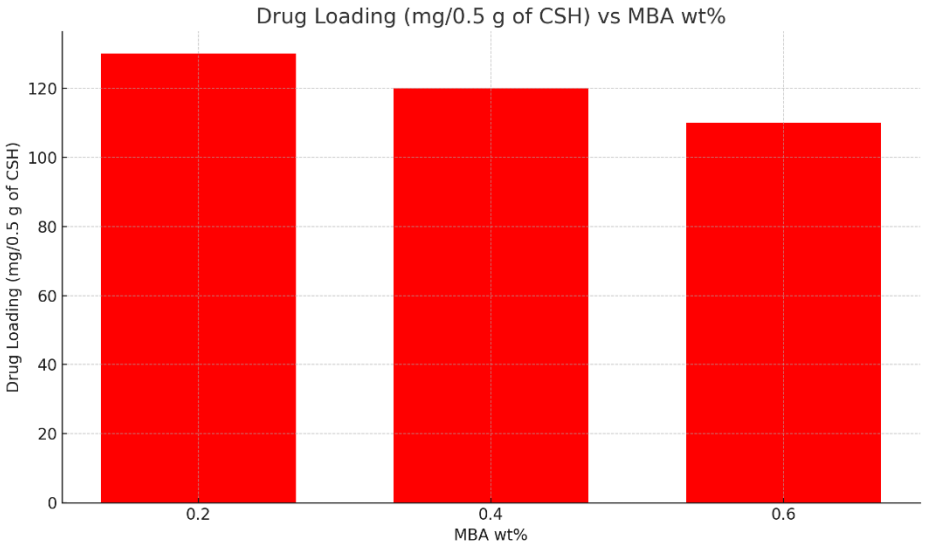

Figure 15. Effect of methylene bisacrylamide (MBA) on drug loading

Carboplatin Release Profile

Carboplatin (CARBP) Release Profile from CSH Hydrogels

The percent release profile of Carboplatin (CARBP) from CSH hydrogels at different pH levels over time is illustrated in Figure 3.10 (a), highlighting the significant impact of pH on drug

release from the hydrogels. This pH-sensitive behavior results in minimal swelling at pH 1.2 and substantial swelling at pH 7.4. At the lower pH of 1.2, the CSH hydrogels exhibit reduced swelling due to the predominance of protonated carboxylic (COOH) groups, which strengthen hydrogen bonding and reduce electrostatic repulsion among COOH groups. Consequently, the hydrogels show decreased swelling and minimal CARBP release.

Conversely, at pH 7.4, increased electrostatic repulsion among negatively charged groups and reduced hydrogen-bonding interactions lead to greater swelling of the hydrogels. This enhanced swelling in a basic pH environment results in a higher release of the drug from the polymeric network. In this study, the fabricated hydrogels demonstrated drug release for up to 24 hours in a phosphate buffer at pH 7.4, with approximately 89% of CARBP released over this period, which is advantageous for targeted delivery of this anticancer agent.

The release of CARBP from the hydrogels is also influenced by the concentrations of the reactants. As the polymer concentration increases, the percent drug release also increases due to the deprotonation of carboxylic and sulfonic groups, as shown in Figure 3.10 (b). However, formulations with higher concentrations of monomer (MAA) and cross-linker (MBA) exhibit slower drug release due to a greater number of unionized carboxylic and sulfonic groups, which decrease electrostatic repulsive forces, as illustrated in Figures 3.10 (c-d). The cumulative percent release of CARBP was approximately 20% at pH 1.2 and 89% at pH 7.4, as depicted in Figure 1. Similar studies by Oprea et al. involving CS and cellulose-based hydrogels loaded with paracetamol and theophylline reported drug release percentages of up to 83%, aligning closely with the 89% release observed in this study (Oprea et al., 2010).

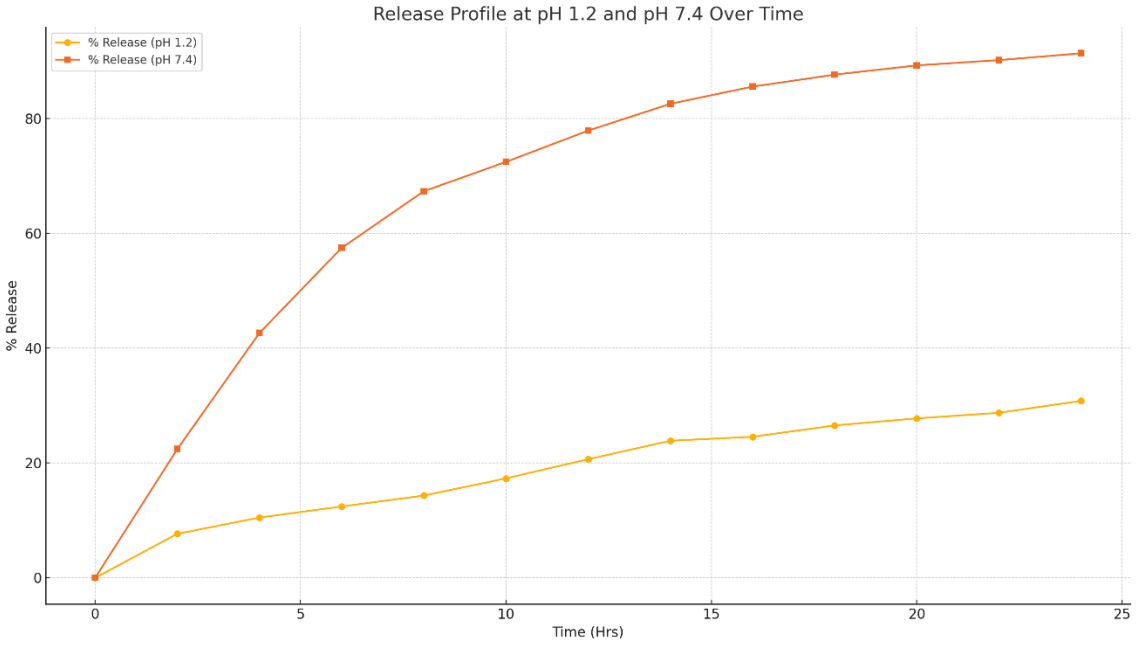

Figure 16. Release of Carboplatin from hydrogel (CSH) in lowerand higher pH medium.

Table 2. Release of Carboplatin from hydrogel (CSH) in lowerand higher pH medium.

Time (Hrs)	% Release (pH 1.2)	% Release (pH 7.4)
0	0	0
2	7.67	22.43
4	10.50	42.67
6	12.43	57.48
8	14.33	67.35
10	17.33	72.46

12	20.66	77.91
14	23.88	82.58
16	24.57	85.57
18	26.55	87.66
20	27.78	89.27
22	28.75	90.19
24	30.83	91.38

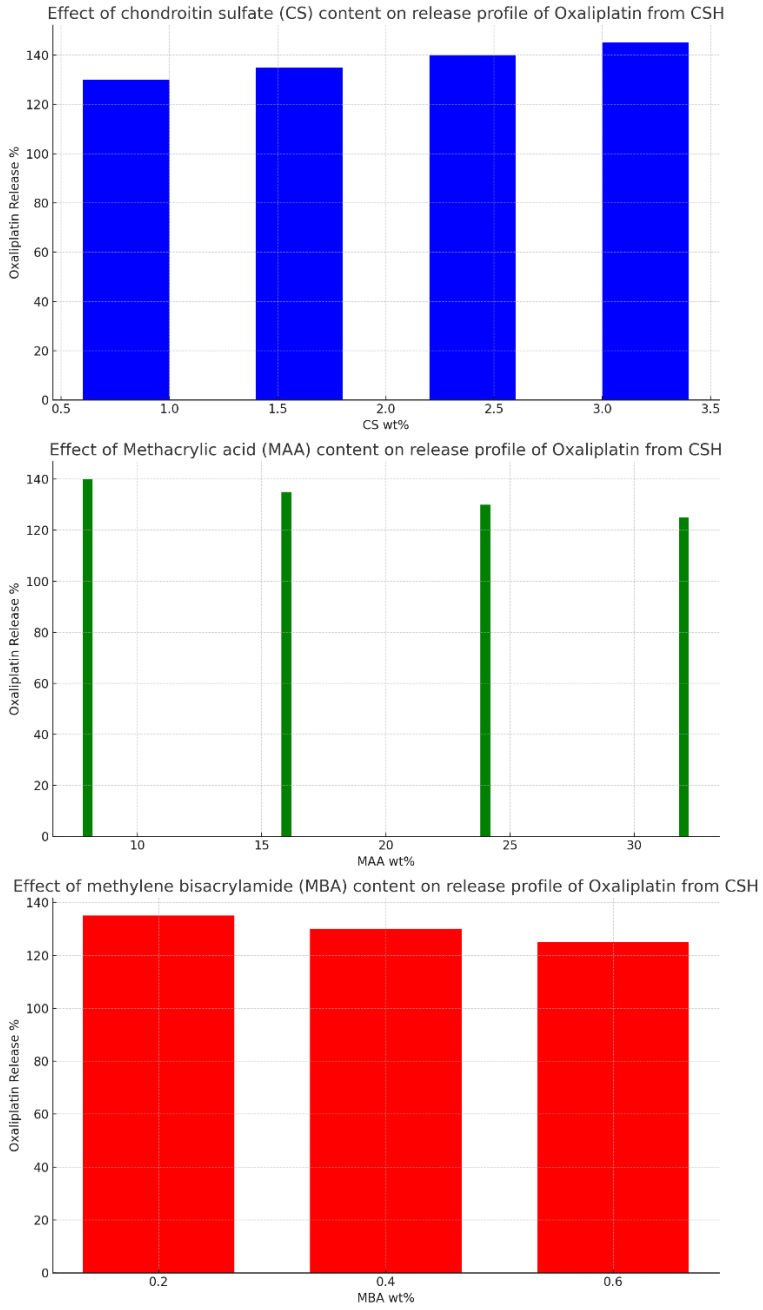

Figure 17. Effect of chondroitin sulfate (CS) content, Methacrylic acid (MAA) content and methylene bisacrylamide (MBA) content on the release profile of Carboplatin.

Kinetic Modeling of Drug Release

Carboplatin (CARBP) release profiles from all CSH hydrogels were evaluated by applying various kinetic models such as zero-order, first-order, Higuchi and Korsmeyer-Peppas models.

The R^2 values, indicating the goodness of fit, and the 'n' value from the Korsmeyer-Peppas model, which provides insight into the drug release mechanism, were key in this analysis. The Zero order model describes a constant drug release rate over time. However, the R^2 values for this model were generally lower compared to the First order model across all formulations. The highest R^2 value for Zero order was 0.8813 for CSH-3, suggesting a moderate fit. This indicates that the Zero order model is not the best fit for these formulations, as the release rate does not remain constant over time. The First order model describes a release rate proportional to the concentration of the drug remaining in the dosage form. The R^2 values for the First order model were consistently high, ranging from 0.91047 (CSH-9) to 0.99447 (CSH-1). This suggests that the drug release from these formulations follows First order kinetics very well, implying that the release rate decreases as the drug is depleted. The Higuchi model explains drug release as a square root of time-dependent process based on Fickian diffusion. The R^2 values for the Higuchi model were relatively high, with most values above 0.87. The highest R^2 value was 0.92063 for CSH-5, indicating a significant role of diffusion in the drug release mechanism. The Korsmeyer-Peppas model is used when the release mechanism is not well known or involves multiple phenomena. The R^2 values for this model were high, indicating a good fit. The 'n' values ranged from 0.498 (CSH-9) to 0.708 (CSH-3), suggesting that most formulations exhibit non-Fickian (anomalous) transport, combining both diffusion and erosion mechanisms. CSH-3, with an 'n' value of 0.708, indicated a stronger tendency towards anomalous transport. Overall, the First order model had the highest R^2 values across all formulations, indicating it as the best fit for describing the release kinetics. This implies that the release rate is dependent on the remaining drug concentration in the dosage form. The Higuchi and Korsmeyer-Peppas models also showed good fits, suggesting significant contributions from diffusion processes. The 'n' values from the Korsmeyer-Peppas model indicated non-Fickian (anomalous) transport mechanisms for most formulations. Among the formulations, CSH-1, CSH-3, and CSH-7 stood out with high R^2 values across multiple models, indicating consistent and predictable release profiles. In particular, CSH-3 showed the highest 'n' value, indicating a more pronounced non-Fickian transport mechanism. Therefore, these formulations exhibit complex release behavior best described by the First order kinetic model, with significant diffusion contributions as indicated by the Higuchi and Korsmeyer-Peppas models.

Table 3. Release Kinetic Modelling of Carboplatin Loaded Hydrogels

Formulations	Zero order R^2	First order R^2	Higuchi R^2	Korsmeyer-Peppas R^2	Korsmeyer-Peppas n
CSH-1	0.8748	0.99447	0.91623	0.97513	0.678
CSH-2	0.8388	0.96497	0.87323	0.93363	0.684
CSH-3	0.8813	0.97747	0.89023	0.96223	0.708
CSH-4	0.7598	0.96607	0.88453	0.91743	0.621
CSH-5	0.7928	0.98617	0.92063	0.95473	0.626
CSH-6	0.7038	0.97177	0.90743	0.92573	0.579
CSH-7	0.8748	0.99017	0.91623	0.97553	0.678
CSH-8	0.6585	0.96847	0.91443	0.92553	0.554
CSH-9	0.4975	0.91047	0.88763	0.95973	0.498

4. CONCLUSION

The development of hydrogels as a delivery system for carboplatin represented a promising advancement in the field of cancer therapeutics. Hydrogels offer numerous advantages, including controlled and sustained drug release, enhanced targeting, reduced systemic toxicity, and excellent biocompatibility. These properties make hydrogels an ideal platform for

improving the efficacy and safety of carboplatin chemotherapy. Incorporating chemical cross-linking between chondroitin sulfate (CS) and methacrylic acid (MAA) has been shown to significantly alter the characteristics of the individual components, resulting in a pH-responsive polymeric network. This network is particularly advantageous for colorectal cancer therapy, where the tumor microenvironment can vary in pH. The cross-linking of CS by methylene bisacrylamide (MBA) imparted substantial strength to the hydrogel, ensured very low water absorption at low pH, and high-water absorption at high pH. This pH-responsive behaviour was critical as it allowed for higher drug release in the more alkaline environments typical of the colorectal cancer microenvironment. The formulated hydrogels not only exhibited pH-responsive behaviour but also demonstrate higher drug release at high pH. This characteristic was especially beneficial for the targeted delivery of carboplatin in colorectal chemotherapy. The observed release profile of carboplatin from these hydrogels confirmed their potential to provide a controlled and efficient delivery mechanism, enhancing the therapeutic outcomes while minimizing the side effects. In conclusion, the fabrication of a chemically cross-linked, pH-responsive polymeric delivery system for carboplatin hold significant promise for colorectal cancer therapies. This approach effectively addressed the limitations of conventional drug delivery methods by combining controlled release, targeted delivery, and biocompatibility.

5. REFERENCES

1. AHMED, E. M. 2015. Hydrogel: Preparation, characterization, and applications: A review. *Journal of Advanced Research,* 6**,** 105-121.
2. ALVARADO-VELEZ, M., PAI, S. B. & BELLAMKONDA, R. V. 2014. Hydrogels as carriers for stem cell transplantation. *IEEE Trans Biomed Eng,* 61**,** 1474-81.
3. ALVAREZ-LORENZO, C. & CONCHEIRO, A. 2014. Smart drug delivery systems: from fundamentals to the clinic. *Chem Commun (Camb),* 50**,** 7743-65.
4. AMINABHAVI, T. M., NADAGOUDA, M. N., JOSHI, S. D. & MORE, U. A. 2014. Guar gum as platform for the oral controlled release of therapeutics. *Expert Opin Drug Deliv,* 11**,** 753-66.
5. CAI, Y., XU, M., YUAN, M., LIU, Z. & YUAN, W. 2014. Developments in human growth hormone preparations: sustained-release, prolonged half-life, novel injection devices, and alternative delivery routes. *Int J Nanomedicine,* 9**,** 3527-38.
6. CALIXTO, G., BERNEGOSSI, J., FONSECA-SANTOS, B. & CHORILLI, M. 2014. Nanotechnology-based drug delivery systems for treatment of oral cancer: a review. *Int J Nanomedicine,* 9**,** 3719-35.
7. KESKIN, D., ZU, G., FORSON, A. M., TROMP, L., SJOLLEMA, J. & VAN RIJN, P. 2021. Nanogels: A novel approach in antimicrobial delivery systems and antimicrobial coatings. *Bioact Mater,* 6**,** 3634-3657.
8. KHALESI, H., LU, W., NISHINARI, K. & FANG, Y. 2021. Fundamentals of composites containing fibrous materials and hydrogels: A review on design and development for food applications. *Food Chem,* 364**,** 130329.
9. KHAYAMBASHI, P., IYER, J., PILLAI, S., UPADHYAY, A., ZHANG, Y. & TRAN, S. D. 2021. Hydrogel Encapsulation of Mesenchymal Stem Cells and Their Derived Exosomes for Tissue Engineering. *Int J Mol Sci,* 22.
10. KHIABANI, S. S., AGHAZADEH, M., RAKHTSHAH, J. & DAVARAN, S. 2021. A review of hydrogel systems based on poly(N-isopropyl acrylamide) for use in the engineering of bone tissues. *Colloids Surf B Biointerfaces,* 208**,** 112035.

11. KHOSRAVIMELAL, S., MOBARAKI, M., EFTEKHARI, S., AHEARNE, M., SEIFALIAN, A. M. & GHOLIPOURMALEKABADI, M. 2021. Hydrogels as Emerging Materials for Cornea Wound Healing. *Small,* 17**,** e2006335.
12. KIM, H. M. & WOO, S. J. 2021. Ocular Drug Delivery to the Retina: Current Innovations and Future Perspectives. *Pharmaceutics,* 13.
13. KIM, S. H., HONG, H., AJITERU, O., SULTAN, M. T., LEE, Y. J., LEE, J. S., LEE, O. J., LEE, H., PARK, H. S., CHOI, K. Y., LEE, J. S., JU, H. W., HONG, I. S. & PARK, C. H. 2021. 3D bioprinted silk fibroin hydrogels for tissue engineering. *Nat Protoc,* 16**,** 5484-5532.
14. LI, J., CHEN, Q., WANG, J., PAN, X. & ZHANG, J. 2021a. Insight Into Bioactive Hydrogels for Wound Healing and Drug Delivery Systems. *Curr Med Chem,* 28**,** 8692-8710.
15. LI, X., YANG, Z., FANG, L., MA, C., ZHAO, Y., LIU, H., CHE, S., ZVYAGIN, A. V., YANG, B. & LIN, Q. 2021b. Hydrogel Composites with Different Dimensional Nanoparticles for Bone Regeneration. *Macromol Rapid Commun,* 42**,** e2100362.
16. LIMA, D. M., CHINELLATO, A. C. & CHAMPEAU, M. 2021. Boron nitride-based nanocomposite hydrogels: preparation, properties and applications. *Soft Matter,* 17**,** 4475-4488.
17. LIMA, T. P. L. & PASSOS, M. F. 2021. Skin wounds, the healing process, and hydrogel-based wound dressings: a short review. *J Biomater Sci Polym Ed,* 32**,** 1910-1925.
18. LIN, H., YIN, C., MO, A. & HONG, G. 2021a. Applications of Hydrogel with Special Physical Properties in Bone and Cartilage Regeneration. *Materials (Basel),* 14.
19. LIN, Q., LIM, J. Y. C., XUE, K., SU, X. & LOH, X. J. 2021b. Polymeric hydrogels as a vitreous replacement strategy in the eye. *Biomaterials,* 268**,** 120547.
20. LIU, J., TIAN, B., LIU, Y. & WAN, J. B. 2021. Cyclodextrin-Containing Hydrogels: A Review of Preparation Method, Drug Delivery, and Degradation Behavior. *Int J Mol Sci,* 22.
21. MÄNNEL, M. J., BAYSAK, E. & THIELE, J. 2021. Fabrication of Microfluidic Devices for Emulsion Formation by Microstereolithography. *Molecules,* 26.
22. MILJKOVIĆ, V., GAJIĆ, I. & NIKOLIĆ, L. 2021. Waste Materials as a Resource for Production of CMC Superabsorbent Hydrogel for Sustainable Agriculture. *Polymers (Basel),* 13.
23. MISRA, R. & ACHARYA, S. 2021. Smart nanotheranostic hydrogels for on-demand cancer management. *Drug Discov Today,* 26**,** 344-359.
24. MO, C., XIANG, L. & CHEN, Y. 2021a. Advances in Injectable and Self-healing Polysaccharide Hydrogel Based on the Schiff Base Reaction. *Macromol Rapid Commun,* 42**,** e2100025.
25. MO, F., JIANG, K., ZHAO, D., WANG, Y., SONG, J. & TAN, W. 2021b. DNA hydrogel-based gene editing and drug delivery systems. *Adv Drug Deliv Rev,* 168**,** 79-98.
26. MOKHTARI, H., TAVAKOLI, S., SAFARPOUR, F., KHARAZIHA, M., BAKHSHESHI-RAD, H. R., RAMAKRISHNA, S. & BERTO, F. 2021. Recent Advances in Chemically-Modified and Hybrid Carrageenan-Based Platforms for Drug Delivery, Wound Healing, and Tissue Engineering. *Polymers (Basel),* 13.
27. MOMIN, M. M. & AFREEN, S. D. 2021. Nanoformulations and Highlights of Clinical Studies for Ocular Drug Delivery Systems: An Overview. *Crit Rev Ther Drug Carrier Syst,* 38**,** 79-107.
28. MONDELO-GARCÍA, C., BANDÍN-VILAR, E., GARCÍA-QUINTANILLA, L., CASTRO-BALADO, A., DEL AMO, E. M., GIL-MARTÍNEZ, M., BLANCO-TEIJEIRO, M. J., GONZÁLEZ-BARCIA, M., ZARRA-FERRO, I., FERNÁNDEZ-

FERREIRO, A. & OTERO-ESPINAR, F. J. 2021. Current Situation and Challenges in Vitreous Substitutes. *Macromol Biosci,* 21**,** e2100066.

29. MORRIS, J., BIETSCH, J., BASHAW, K. & WANG, G. 2021. Recently Developed Carbohydrate Based Gelators and Their Applications. *Gels,* 7.
30. MOSTAKHDEMIN, M., NAND, A. & RAMEZANI, M. 2021. Articular and Artificial Cartilage, Characteristics, Properties and Testing Approaches-A Review. *Polymers (Basel),* 13.
31. NONOYAMA, T. & GONG, J. P. 2015. Double-network hydrogel and its potential biomedical application: A review. *Proc Inst Mech Eng H,* 229**,** 853-63.
32. SABERIAN, M. & ABAK, N. 2024. Hydrogel-mediated delivery of platelet-derived exosomes: Innovations in tissue engineering. *Heliyon,* 10**,** e24584.
33. SARKAR, S., KUMAR, R. & MATSON, J. B. 2024. Hydrogels for Gasotransmitter Delivery: Nitric Oxide, Carbon Monoxide, and Hydrogen Sulfide. *Macromol Biosci,* 24**,** e2300138.
34. SGHIER, K., MUR, M., VEIGA, F., PAIVA-SANTOS, A. C. & PIRES, P. C. 2024. Novel Therapeutic Hybrid Systems Using Hydrogels and Nanotechnology: A Focus on Nanoemulgels for the Treatment of Skin Diseases. *Gels,* 10.